

Structural energy-volume relations in first-row transition metals

A. T. Paxton*

*Max-Planck-Institut für Festkörperforschung, Heisenbergstrasse 1, Postfach 80 06 65,
D-7000 Stuttgart 80, Federal Republic of Germany*

M. Methfessel and H. M. Polatoglou[†]

Fritz-Haber-Institut, Faradayweg 4-6, D-1000 Berlin 33, Federal Republic of Germany

(Received 29 November 1989)

The total energy of the 3*d* transition metals is calculated as a function of volume in each of six different crystal structures. The calculations employ the local-density-functional scheme and the full-potential linear muffin-tin orbitals method. Both self-consistent and non-self-consistent Harris-Foulkes calculations are shown and the connection is made between these and simpler tight-binding and classical models of interatomic forces. The energy-volume relations may serve as a database in the construction of such empirical schemes.

I. INTRODUCTION

In this paper, we show calculated energy-volume (E - V) curves for the first-row transition metals from Sc to Cu. We not only compare the energies of the cubic (fcc) and hexagonal (hcp) close-packed and body-centered-cubic (bcc) phases, but also investigate the stability of mythical structures with coordination numbers between 4 and 8. The purpose of the exercise is threefold. (1) By showing E - V curves calculated using a state-of-the-art Hohenberg-Kohn density-functional approach in the Kohn-Sham local-density approximation^{1,2} we are able to provide benchmark calculations against which to compare empirically obtained interatomic force potentials used in materials simulation. (2) The benchmark curves are used here as a test of the recently developed and much-discussed Harris-Foulkes approximation³⁻⁵ to the self-consistent Hohenberg-Kohn energy functional. (3) We are able to confirm the predictions of relative stability of the close-packed and bcc phases from canonical d -band theory⁶ and tight-binding models, discuss the connection between the Harris-Foulkes approximation and the tight-binding bond model,⁷⁻⁹ and use our results to assess the possible transferability of tight-binding parameters for transition metals into undercoordinated defect environments.

Approximate descriptions of the bonding in transition metals have existed (to varying degrees of complexity) in the literature for some 30 years (see, for example, Refs. 10, 9, and 11). It is now known that while pair potentials have proved enormously useful in understanding phenomena ranging from radiation damage¹² to the structure of extended defects,^{13,14} a proper treatment of the problem must go beyond this to include the important effect of d -band filling which dominates the trends in properties across the transition series; we also know that the simplest d -band tight-binding model is itself in error due to

neglect of the effects of the sp band. An additional complication is the magnetic ground state of transition metals near the end of the row. In a spin-polarized description, the fcc and hcp density of states (DOS) in Ni and Co are split because their Fermi level falls in a large maximum and the Stoner parameter is large; bcc Fe is stabilized by a large splitting of the DOS so that the Fermi level for one of the spins falls in the minimum separating the bonding and antibonding states characteristic of the bcc DOS, while the opposite spins occupy an almost full d band. It is not clear whether even the local-spin-density-functional theory can correctly predict the bcc structure of α -Fe (Ref. 15) or the complicated spin and crystal structures of Cr and Mn. Furthermore, no simple model can include magnetic effects easily, so we have chosen to make our calculations non-spin-polarized. Naturally, an empirical potential for Fe, say, must produce a bcc ground state; however it is worthwhile emphasizing that in the local-density approximation, its structure is hcp.

For calculating the structures of extended defects such as surfaces, grain boundaries, dislocations, and cracks, as well as problems of point defect formation and migration energies, it is important that an empirical description of bonding should not fail in situations where atoms are undercoordinated. This has always been a drawback in tight-binding or classical potentials for semiconductors, and it is not clear whether a tight-binding description for transition metals would not also fail. As a rough estimate of how the energy might change with undercoordination, we have looked at the simple hexagonal, simple cubic, and diamond cubic structures in which atoms have, respectively, eight, six, and four neighbors.

The organization of the paper is as follows. In Sec. II, we briefly outline the method we have used to solve the Schrödinger equation self-consistently, discuss the sources of error, and estimate the accuracy of the present calculations. We show results for the close-packed

phases in Sec. III which we compare with previous local-density and tight-binding predictions and give a brief discussion of the effects of d -band magnetism. The E - V curves are presented in Sec. IV, and results using the Harris-Foulkes approximation in Sec. V. The axial ratio of the hcp metals is discussed in Sec. VI. We make contact again with tight-binding theory in Sec. VII, where all the E - V data points are scaled to the Rose equation of state and the analysis of Spanjaard and Desjonquères is used to assess the transferability of tight-binding parameters. Discussion and conclusions can be found in Sec. VIII.

II. METHOD OF CALCULATION

A. Full-potential LMTO

We solve the Schrödinger equation for each crystal structure at a number of volumes, self-consistently within the local-density approximation² (LDA). The Hamiltonian is represented in a basis of linear muffin-tin orbitals¹⁶ (LMTO's) which are augmented with numerical solutions of the radial Schrödinger equation within nonoverlapping muffin-tin spheres. No shape approximation for the potential or charge density is used. In the interstitial region, these quantities are expressed in Hankel-function expansions using a recently developed approach.¹⁷ This method is not much slower than standard LMTO calculations in the atomic-spheres approximation^{18,19} (ASA). Because the augmentation is done in somewhat smaller spheres than in the LMTO-ASA method, it is necessary to include two basis functions in each angular momentum l channel. These are chosen to have kinetic energies of 0 (as do conventional LMTO's) and -1 Ry. The basis thus consists of 18 functions per atom. The core is permitted to relax but is taken to be spherical.

In the linear method, we are restricted to one principal quantum number in each l channel in the band calculation. However, in the first-row transition metals—particularly at the beginning of the series and in the non-close-packed structures—the $3p$ electrons spill out of the muffin-tin spheres and can show non-negligible dispersion; even $3s$ electrons can be affected in extreme cases such as the diamond cubic structure. These “semicore” electrons from low-lying bands separated from the valence bands by an energy gap. We have treated the semicore states in the same way as the band states, by setting up and diagonalizing the Hamiltonian a second time. This automatically corrects errors in the eigenvalues and charge density due to the wave functions extending into the interstitial region and into neighboring spheres. In the “second-panel” band calculation we use only an sp basis, and since the bands are quite flat and completely filled, only a few (special²⁰) \mathbf{k} points are needed in accumulating the eigenvalue sum. An alternative method of dealing with semicore states has been discussed by Mattheiss and Hamann.²¹

B. Sources of error and assessment of accuracy

Sources of error fall naturally into two categories: approximations arising in the construction of a model to represent the solid state, and those arising from the execution of the model. The use of local-density-functional theory in calculating structural properties of transition metals has been addressed in the literature^{22,21,23–26} and will be discussed in the present context briefly in Sec. III. Aside from the LDA, our model assumes that the full-potential LMTO method¹⁷ with a basis of 18 orbitals per atom is suitably accurate for the present purpose. Possible sources of error are approximations made in the calculation of the interstitial charge density, and exchange-correlation energy density and potential, and have been assessed in some detail recently.²⁷ The charge density is calculated exactly in the muffin-tin spheres in angular momentum components up to $l=4$. We use the same angular momentum cutoff in the interpolation of quantities in the interstitial region,¹⁷ expanded in Hankel functions of energies -1 and -3 Ry. A measure of the errors in this procedure is given by the dependence of the total energy on the kinetic energies (i.e., the localizations) of the charge-density basis set. In the close-packed metals, varying the energies from $(-1, -3)$ Ry to $(-0.1, -1)$ Ry leads to total energy changes of less than 0.1 mRy per atom. Errors arising from the size of the basis are easy to assess:²⁷ in the present instance, the total energy is absolutely converged to within a few mRy per atom. This is a far smaller error than that made by the LDA, in particular in calculating the energies of free atoms.²² Furthermore, this small error is known to cancel in the calculation of energy differences between different crystal structures.

Convergence in the eigenvalue sums falls into the second category mentioned at the beginning of this section, and is a consequence of the need to evaluate integrals over the Brillouin zone. We use a uniform mesh of sampling points with at least 15 divisions along each of the primitive vectors. In cubic lattices we shift this mesh into “special points”²⁰ positions so as to decrease the degeneracy of each point and hence minimize the total number of sampling points. In conventional sampling,²⁴ a complementary error function of width W replaces the step function at the Fermi surface so as to ensure exponential convergence with the number of divisions. We use a recently developed generalization of this,²⁸ in which we approximate the step function by a complementary error function plus N higher-order correction terms. The width parameter W and the order N are determined by stringent convergence tests in typical cases and subsequently estimated by the amount of variation in the DOS near the Fermi energy. We find that in self-consistent calculations the total energy is less sensitive to the choice of W and N than in the problem of integrating a given set of bands. This is apparently a consequence of the variational principle, and means that a choice of N and W by inspection is appropriate here. A more careful choice of these parameters can lead to a very large saving in non-self-consistent methods, such as frozen potential or Harris-Foulkes calculations. We estimate that our

Brillouin-zone integrals are converged absolutely to within 0.5 mRy.

III. STRUCTURAL ENERGY VERSUS BANDFILLING IN THE CLOSE-PACKED PHASES

We begin the presentation of our results with the energies of the close-packed structures, fcc, hcp, and bcc. There is a long tradition of the calculation of the close-packed structural energy differences as a function of atomic number in the three transition series.²⁹⁻³³ This has arisen from the curiosity evoked by the observation that the transition metals follow a consistent trend hcp→bcc→hcp→fcc across each of the three series, with the only exceptions being La, Mn and the ferromagnetic elements Fe and Co. Friedel³⁴ first suggested that the structural energy of the transition metals was dominated by the eigenvalue sum or bond energy arising from the narrow band of *d* electrons. This suggestion was partly motivated by the observation that the sublimation energies followed a parabolic development across the series as did the cohesive energy in the Hartree approximation,^{35,36}

$$\int_{-\infty}^{E_F} (\varepsilon_d - E) n_d(E) dE ,$$

for any reasonable shape of the *d*-electron density of states n_d (centered at the atomic energy level ε_d) including the very simple rectangular DOS.^{34,37} Developing n_d in its power moments,

$$\mu_r = \int_{-\infty}^{\infty} (E - \varepsilon_d)^r n_d(E) dE ,$$

Ducastelle and Cyrot-Lackmann³⁰ showed the direct connection between these moments and the lattice topology. Exploiting the fivefold degeneracy of the *d* band, and transformation rules given in the Slater-Koster tables,³⁸ they gave the exact result that within the tight-binding model, the fcc-hcp energy difference would go through zero at least twice as a function of the filling of the *d* band. This follows from the first four moments ($\mu_0 - \mu_3$) being identical in the two structures. Furthermore, using only the difference between the first nonidentical moment μ_4 for each structure, they were able to immediately sketch the general shape of the fcc-hcp energy-difference curve as a function of number of *d* electrons. The characteristic separation of the bcc DOS into predominantly T_{2g} bonding and predominantly E_g antibonding states by a pseudogap immediately leads to the prediction that the bcc structure will be stabilized in the center of the transition series, i.e., near half band filling. Using just eight exact moments of the DOS of a canonical *d* band⁶ in a first-neighbor model (first and second in bcc) already gives enough detail to the shapes derived from the above simple arguments to reproduce the structural trends (with the exceptions of incorrectly predicting the bcc structure for the noble metals in which the *s*-electrons are playing a major role in cohesion, and moving the second zero in the fcc-bcc curve to too large a band filling, hence giving the bcc structure to the hcp metals in group 8).³³

The first calculation of these structural energy

differences in the LDA was by Skriver,³⁹ who used LMTO-ASA in the force theorem developed by Andersen.⁴⁰ Here, only one structure (fcc) is made self-consistent. The resulting atomic-sphere potentials are then used to construct a trial potential for the second structure. The structural energy difference is then the difference in eigenvalue sum of the self-consistent structure and that obtained from solving the Kohn-Sham equation in the trial potential. There is a clear connection between this simplified (but in many cases accurate) LDA approach and the association of the structural energy difference with Friedel's bond energy. A comparison shows⁴¹ that the canonical moments method is in good qualitative agreement with the LDA force theorem results. In Fig. 1, we show the structural energy differences we have been discussing, calculated self-consistently in the full-potential LMTO method outlined in Sec. II. We compare these with the results of Skriver³⁹ for the first-row metals.

Although it is clear that the structure of these curves can be easily predicted from simple tight-binding models, the fact that the actual energy differences are very small means that great care must be taken when making these calculations from first principles. In fact, the fcc-hcp energy differences are on the order of the absolute accuracy of first-principles methods, so it is gratifying that we are in such good agreement with the calculations of Skriver in the ASA force theorem. Indeed, many of the differences that remain are due to the fact that while Skriver³⁹ used an ideal axial ratio for all his hcp structures, we have chosen to use experimental values for those metals (Sc and Ti) whose observed ground-state structure is hcp. Also we have calculated the energy differences at our calculated atomic volumes rather than at experimental ones.

Let us comment briefly on the results. The structures of the nonmagnetic elements Sc, Ti, and V are correctly reproduced, as well as that of Cr, where the half filling of the *d* band dominates over magnetic effects in stabilizing the bcc structure. The local-density prediction of the

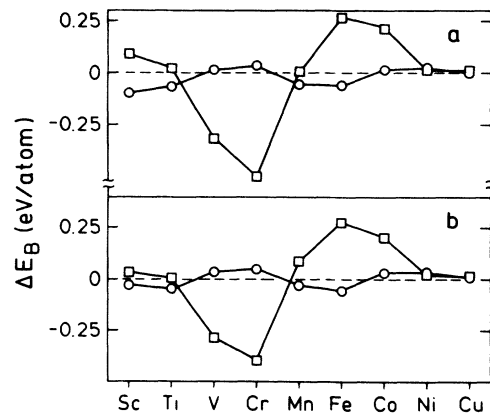


FIG. 1. hcp-fcc (circles) and bcc-fcc (squares) structural energy differences in the 3*d* transition metals. (a) present results using full-potential LMTO; (b) Skriver's calculations using LMTO-ASA and the force theorem.

structure of Mn and Fe is hcp. In the observed ground state Mn has the structure of the “ χ ” phase,⁴² a body-centered-cubic structure with 58 atoms per cell. The structure is almost topologically close packed.^{42,43} Of the 29 atoms in the primitive cell, there are four inequivalent positions populated by 1, 4, 12, and 12 atoms, respectively. Five atoms are in CN16 (i.e., with a coordination number of 16) coordination polyhedra, 12 in CN12 icosahedra, and 12 have 13 neighbors in their coordination shells. Experimentally,⁴⁴ it is found that the Mn atoms in CN16 polyhedra have a large (spin up) local magnetic moment, while the remaining 24 atoms have a smaller (spin down) moment such that the total antiferromagnetic moment is zero. Topological close packing is the most efficient way of close packing two atoms of different sizes. In α -Mn, the high-spin atom behaves as the large atom, and the low-spin atom as the small atom: the magnetic structure seems consistent with the atomic structure of the χ phase in which the higher coordinated sites tend to be occupied by the larger atom.⁴² It is not clear at present, though, why this structure should be favored over simpler close-packed structures, for example, the antiferromagnetic bcc δ -Mn. Ferromagnetic α -Fe is, of course, well known to have the bcc structure in the ground state. Nonmagnetic hcp Fe, however, is thought⁴⁵ to have a lower enthalpy than fcc below 400 K, which is consistent with the present results. Also α -Fe begins to transform to hcp ϵ -Fe at 130 kBar,⁴⁶ although at this pressure the magnetic moment will still be larger than 2 Bohr magnetons^{22,47} so it cannot be the vanishing of the moment that stabilizes the hcp phase. LMTO-ASA calculations¹⁵ in the local-spin-density approximation with gradient corrections to the exchange-correlation energy density⁴⁸ show a phase transformation from ferromagnetic α -Fe to nonmagnetic fcc at about 80 kBar. These authors¹⁵ did not consider the hcp phase, but their results must be an upper bound on the α - ϵ transformation pressure in their model. Our nonmagnetic calculations incorrectly give Co the fcc structure, although below 700 K Co is hcp.⁴⁹ In fact, both phases are observed at room temperature, and it has been speculated⁴⁹ that fcc is in fact the stable phase. It remains to be seen whether the ground-state structure of Co can be calculated from first principles; we return to this point briefly in Sec. VI. The fcc structure of Ni is correctly predicted in the LDA. hcp Ni has been observed in thin films subjected to heat treatment,⁵⁰ and electron⁵¹ and neutron irradiation.⁵² However, there seems to be no evidence of the existence of hcp Ni in a bulk phase. Finally, it is interesting to note that the structural energy differences in Cu are extremely small. Cu lies beyond the realm of d -band tight-binding theory, but it seems that in the LDA, the energies of hcp and fcc phases in Cu [and Ag (Ref. 25)] are almost indistinguishable.

IV. ENERGY-VOLUME RELATIONS

We now turn to our calculated E - V curves in the first-row transition metals. Curves of this kind were first produced for Si in an historic paper by Yin and Cohen⁵³ using local-density theory in a plane-wave, first-principles

pseudopotential calculation. These curves were originally intended to demonstrate the power of the LDA in predicting structural phase stability and pressure-induced transformations in Si. However, they also became standard benchmark results against which classical⁵⁴ or semiempirical tight-binding⁵⁵ models could be tested. In some cases they have actually been used in *fitting* the parameters of the models.⁵⁶

In view of this, and the increasing interest in the creation of classical and semiempirical potentials for transition metals, we show in Fig. 2, E - V data points for the elements Sc–Cu, each in six structure: fcc, hcp, bcc, simple hexagonal (sh), simple cubic (sc), and diamond cubic (dc). We have drawn curves by hand through the calculated data points. For those elements for whom the close-packed structural energy differences are close to zero, we show additional curves in insets with expanded scales. We should note, however, that on these scales the separation of the curves approaches the accuracy of our calculations (see Sec. III). We have omitted the hcp curves in V, Ni, and Cu. In V, the two curves become superimposed at $\Omega/\Omega_0 < 0.9$ (see also Fig. 3). hcp Ni will be discussed in Sec. VI. The energy difference between ideal axial ratio hcp and fcc Cu is less than 0.007 eV/atom in our calculations. We do, however, find fcc Cu to be stable by this amount with respect to ideal axial ratio hcp.

The energies shown in Fig. 1 are binding energies per atom E_B relative to the energies of spin-polarized free atoms. The free-atom energies are identical to those given by Moruzzi, Janak, and Williams²² since we have used their parameterization of the von Barth–Hedin exchange-correlation energy density. The atomic volumes are given relative to the observed atomic volumes in the ground state; these volumes are given in Table I. In the same table, we show our calculated atomic volumes Ω_{\min} , cohesive energies, and bulk moduli K_0 obtained from least-squares analyses of the E - V data points. We will comment briefly on these results; they may be compared to a similar compilation by Moruzzi, Janak, and Williams,²² who pioneered these calculations using the Korringa-Kohn-Rostoker (KKR) method. (We have neglected corrections for zero-point motion in our calculations.²²) The cohesive energies ($E_{\text{coh}} = -E_B$) are well known to be consistently overestimated in the LDA.²² This is most probably largely due to errors made in calculating the total energy of free atoms. However, it is useful to know what the LDA values of cohesive energy are, and to compare these to more approximate calculations. Ω_{\min} and K_0 are, respectively, underestimated and overestimated in the LDA. In fact, we find that our bulk moduli are also mostly higher than those found by Moruzzi, Janak, and Williams,²² although both are quoted at the calculated atomic volume.⁵⁷ In the magnetic metals, the magnetic moment favors larger atomic volumes, and hence the errors in Ω_{\min} and K_0 are particularly large in these elements in the present non-spin-polarized calculations. A direct comparison to experimental quantities for magnetic materials is not very relevant and is included in Table I for completeness and for comparison with previously published calculations.²²

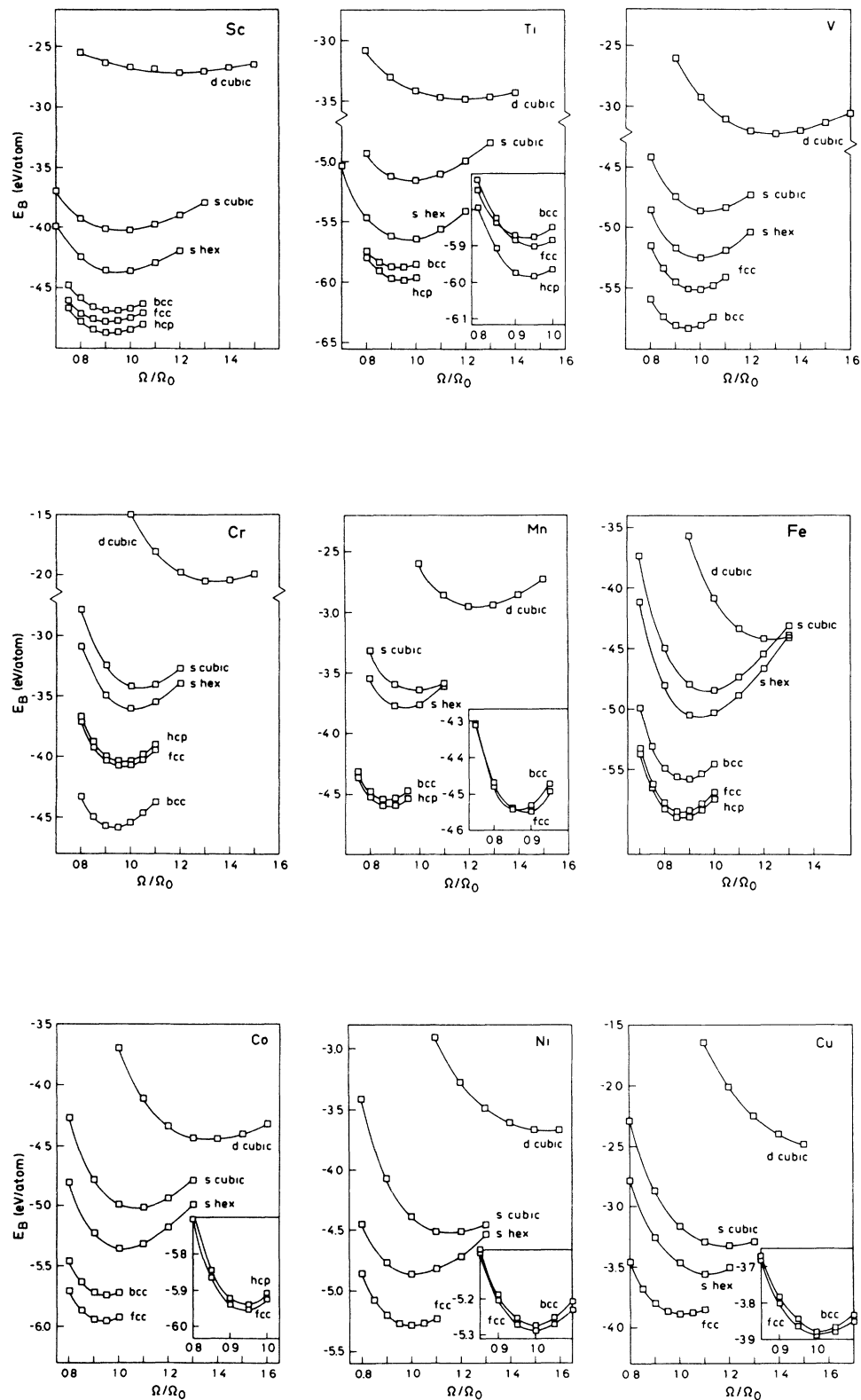


FIG. 2. Self-consistent, full-potential LMTO structural energy-volume curves in the $3d$ transition metals: binding energy (eV) vs atomic volume Ω normalized to the experimental atomic volume Ω_0 . Structures are fcc, hcp, bcc, simple hexagonal, simple cubic, and diamond cubic.

TABLE I. Self-consistent, ground-state properties of the 3d metals. Ω_0 is the reference atomic volume and the experimental cohesive energy E_{coh} and bulk modulus K_T are taken from Kittel's book [C. Kittel, *Introduction to Solid State Physics*, 5th ed. (Wiley, New York, 1976)].

Element	Structure	Ω_0 (\AA^3)	$\Omega_{\text{min}}/\Omega_0$	E_{coh} (eV/atom)		K_T (Mbar)	
				Theory	Expt.	Theory	Expt.
Sc	hcp	25.00	0.92	4.87	3.90	0.6	0.44
Ti	hcp	17.65	0.95	5.98	4.85	1.2	1.05
V	bcc	13.83	0.94	5.83	5.31	2.0	1.62
Cr	bcc	12.01	0.93	4.58	4.10	2.8	1.90
Mn	hcp	12.21	0.87	4.61	2.92	2.9	0.60
Fe	hcp	11.80	0.87	5.90	4.28	3.0	1.68
Co	fcc	11.06	0.94	5.96	4.39	2.6	1.91
Ni	fcc	10.90	1.00	5.29	4.44	2.0	1.86
Cu	fcc	11.81	1.01	3.89	3.49	1.6	1.37

V. THE HARRIS-FOULKES APPROXIMATION

One of the most expensive or time-consuming aspects of the density functional method is the need to proceed with the calculation to self-consistency. This was the motivation for Harris³ to develop his approximate energy functional. Independently, Foulkes⁴ discovered the same functional in a study of the relationship between density-functional and tight-binding theories.⁵ The Hohenberg-Kohn¹ total energy is, as usual, separated into a noninteracting kinetic energy term T_s and an electrostatic term F , both functionals of the self-consistent charge density n_0 :

$$E[n_0] = T_s[n_0] + F[n_0],$$

and if ϵ_i are the eigenvalues of the self-consistent Kohn-Sham² problem, then

$$E[n_0] = \sum_{i,\text{occ}} \epsilon_i - \int \frac{\delta F[n_0]}{\delta n} n_0 + F[n_0].$$

The Harris-Foulkes (HF) total energy is a functional only of a trial input density n_{in} :

$$\begin{aligned} E_{\text{HF}}[n_{\text{in}}] &\equiv \sum_{i,\text{occ}} \tilde{\epsilon}_i - \int \frac{\delta F[n_{\text{in}}]}{\delta n} n_{\text{in}} + F[n_{\text{in}}] \\ &= E[n_0] + \frac{1}{2} \int \int \frac{\delta^2 E[n_0]}{\delta n^2} (n_{\text{in}} - n_0) \\ &\quad \times (n_{\text{out}} - n_0) + \dots, \end{aligned}$$

where $\tilde{\epsilon}_i$ and n_{out} are the eigenvalues and charge density obtained from solution of the Kohn-Sham equations with effective potential $\delta F[n_{\text{in}}]/\delta n$. The HF functional is seen here to have the following properties. (i) It is identical to

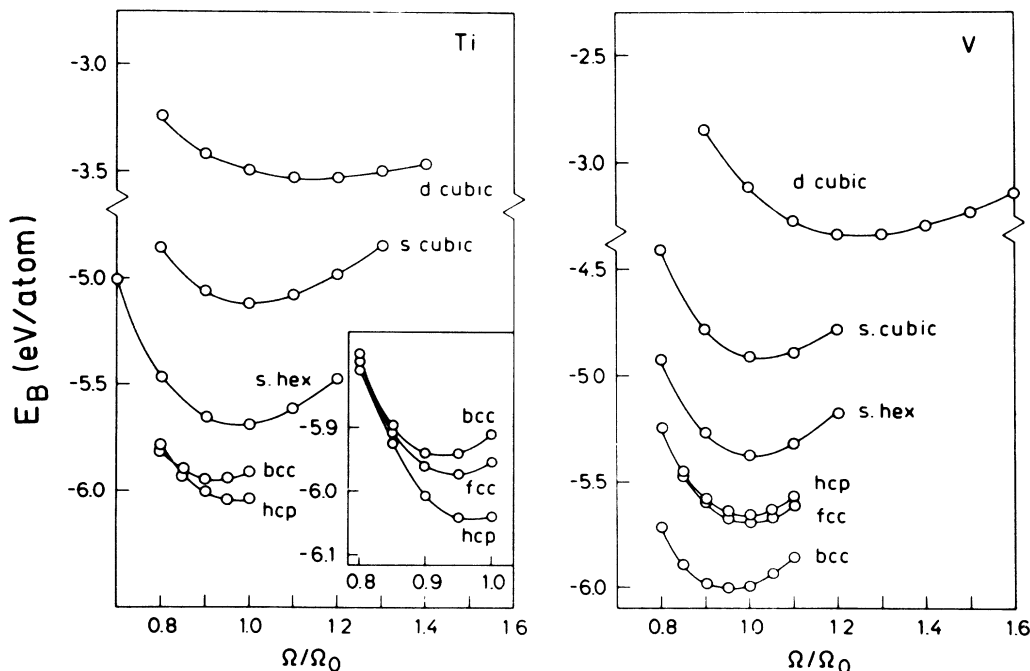


FIG. 3. Structural energy-volume curves for Ti and V in the Harris-Foulkes approximation. Axes as in Fig. 2.

the Hohenberg-Kohn functional when $n_{in} = n_0$. (ii) For a given trial density, the HF total energy is equal to the self-consistent total energy to second order. As a consequence, E_{HF} is stationary (but not necessarily minimal) at n_0 .

The HF approximation is only one in a class of non-self-consistent density-functional methods exploiting the variational principle. These include the non-self-consistent procedure based on the Hohenberg-Kohn functional⁵⁸ (recently reviewed and compared with the HF approximation^{59,60}) and methods based on the force theorem.^{61,40} The HF approximation is especially appealing in the present context because of its close connection with tight-binding theory as developed by Foulkes^{4,5} and Sutton *et al.*⁷ Furthermore, the HF approximation has in the recent past been shown to be remarkably successful in reproducing self-consistent calculations of structural properties of elements and compounds.⁶² We have found similarly excellent agreement between self-consistent and HF calculations in the present study of transition metals.

The procedure we have followed is the same as that of Polatoglou and Methfessel,⁶² except that we remove the shape approximation of the ASA. Details can be found in Ref. 60. There is then a close connection between our implementations of the self-consistent and non-self-consistent problems. Our trial density is a superposition of overlapping, self-consistent free-atom densities. (We use an s^2d^n atomic configuration.) From this density, we construct an effective Kohn-Sham potential exactly as in the self-consistent calculations, following the same procedure for the solution of the Schrödinger equation.¹⁷ The sum of occupied eigenvalues is added to the “double counting” terms evaluated for the input density. We may choose to stop here or accumulate n_{out} and continue to self-consistency to obtain the Hohenberg-Kohn total energy.

For brevity, we concentrate on results for Ti and V, and show in Fig. 3 their $E-V$ relations, and give in Table II a detailed tabulation of properties for all six structures. Figure 3 and Table II may be used to compare directly the HF with the self-consistent results. The equilibrium

atomic volumes are generally overestimated; the bulk moduli are very similar to the self-consistent values. (We have estimated the bulk moduli at the minimum of the Harris-Foulkes $E-V$ curves.) Absolute cohesive energies are also overestimated in almost all cases. We find this to be a general trend for the transition metals in the first row. This is possible because E_{HF} is a stationary but not necessarily variational estimate of the total energy⁵ as mentioned above. An improvement in the total energy can be made by renormalizing the trial atomic density,^{63,59} but for simplicity we have not attempted this here.

VI. AXIAL RATIO OF hcp TRANSITION METALS

It would have been desirable to minimize the self-consistent total energy in the hcp structures with respect to the axial ratio as well as the atomic volume. It has already been shown in the case of Si that the full-potential LMTO method is capable of accurately reproducing the change in total energy with lattice distortions, even up to third order in the strain.^{17,27} Nevertheless, we have chosen to use ideal axial ratios in all metals except Sc and Ti, where we have used experimental values. Apart from the expense involved, we find that nonmagnetic Fe, Co, and Ni are mechanically unstable with respect to a rhombohedral c/a distortion. This is a Peierls instability driven by the very flat d bands at the Fermi surface characteristic of the fcc and hcp band structures. (This effect is of course removed in the magnetic electronic structure by shifting the nondegenerate spin bands up and down with respect to the Fermi energy.) No doubt, the fcc structure would also distort into a rhombohedral lattice, but because the fcc structure is at a symmetry dictated energy extremum with respect to rhombohedral distortion, it is admissible to calculate its total energy. The hcp structure with ideal axial ratio is at no such extremum, and we therefore tentatively have shown $E-V$ curves for hcp Fe and Co (especially since the hcp-fcc phase transformation in Co is of interest) but not in Ni, where the instability is strongest. We also remark that in stable hcp structures, we find the energy change involved

TABLE II. Comparison of equilibrium volume, cohesive energy, and bulk modulus between self-consistent (SC) calculations and the Harris-Foulkes (HF) approximation. We use Ti and V as examples and show results from all six phases studied.

Element	Structure	Ω_{min}/Ω_0		E_{coh} (eV/atom)		K_0 (Mbar)	
		SC	HF	SC	HF	SC	HF
Ti	fcc	0.91	0.94	5.92	5.97	1.2	1.1
	hcp	0.95	0.97	5.98	6.04	1.2	1.1
	bcc	0.90	0.92	5.89	5.94	1.2	1.1
	sh	0.96	0.97	5.65	5.69	1.0	1.0
	sc	0.98	1.00	5.16	5.12	0.9	0.8
	dc	1.19	1.13	3.48	3.53	0.3	0.3
V	fcc	0.98	1.00	5.51	5.69	1.9	1.9
	hcp	0.98	0.99	5.50	5.66	1.9	1.9
	bcc	0.94	0.95	5.83	6.01	2.0	2.0
	sh	1.00	1.01	5.25	3.37	1.6	1.7
	sc	1.03	1.03	4.87	4.92	1.4	1.5
	dc	1.29	1.25	3.22	3.34	0.8	0.7

in minimizing the axial ratio is of the order of 1 mRy per atom (see also Ref. 26) which is undetectable on the scale of Fig. 2. In noble metals, the variation is almost ten times smaller:²⁵ such a change is unlikely to be sufficient to stabilize hcp Cu with respect to fcc; however, we have not attempted the calculation.

Notwithstanding the above remarks, some comments on the axial ratio in hcp transition metals are in order. Ducastelle and Cyrot-Lackmann³⁰ have proved (again, as described in Sec. IV, using the fourth-moment degenerate d -band model) the following remarkable result. Transition metals for which the fcc-hcp energy difference is negative will further lower their energy by a reduction in axial ratio. Conversely, in those metals whose fcc phase is stable with respect to hcp, the hcp structure *would* distort so as to increase its axial ratio. The same result was found numerically by Finnis,^{8,7,9} who calculated the $(dd\sigma)$, $(dd\pi)$, and $(dd\delta)$ bond orders in the canonical d -band model as a function of band filling. In the hcp structure, the six bonds parallel to the close-packed (0001) planes are inequivalent to the six out-of-plane bonds. Finnis found that the ratio of the in-plane to out-of-plane $(dd\pi)$ bond orders was < 1 around band fillings of 1 and 2 d electrons (corresponding to Sc and Ti) and 5 and 6 (Mn and Fe), and > 1 elsewhere. The result is that, since in the tight-binding bond model the interatomic force is proportional to the bond order,⁸ in the former case the interatomic forces would act to shorten the out-of-plane bonds and hence lower the axial ratio, and *vice versa*, exactly as predicted by Ducastelle and Cyrot-Lackmann.³⁰

Considering the connection between the HF and tight-binding bond models, it would be disappointing if this effect were not reproduced in the HF approximation. Table III shows that for Sc, Ti, and V the prediction is indeed confirmed. Moreover the axial ratios in Sc and Ti are in satisfactory agreement with experiment.

The tight-binding picture of the axial ratio is remarkably well supported in the axial ratios of metastable hcp metals. The α - ϵ phase transformation⁴⁶ in Fe is rather sluggish, but on its completion at about 300 kBar ($\Omega/\Omega_0=0.88$), the axial ratio is 1.59, having quite strongly decreased with pressure as the hcp phase becomes more stable. hcp Ni is almost certainly unstable—thin films grown electrolytically on hcp Co transform to the fcc structure when removed from their substrates⁶⁴—and its axial ratio^{52,50,51} is 1.65 (larger than ideal 1.633). In Co, the axial ratio is 1.632; this implies that hcp is marginally stable with respect to fcc, contrary to our LDA result and the speculation of Troiano and Tokich.⁴⁹

TABLE III. Hexagonal axial c/a ratio for Sc, Ti, and V calculated in the Harris-Foulkes approximation and compared to the experimental values.

Element	HF	Axial ratio	Expt.
Sc	1.57		1.594
Ti	1.59		1.587
V	1.65		

VII. UNIVERSAL FEATURES OF THE ENERGY-VOLUME RELATIONS

A. The zero-temperature equation of state

In a recent series of papers,^{65,66} by examining a large database of theoretical and experimental findings, Rose and co-workers have found that in a wide variety of instances, energy-length relationships have a universal shape. This has become known as the “Rose equation of state” and takes the form

$$\frac{E(a)}{E_{\text{coh}}} \equiv E^*(a^*) = p(a^*)e^{-a^*} \approx -(1+a^*)e^{-a^*},$$

where p is a polynomial and⁶⁶

$$p(a^*) = -1 - a^* - 0.05(a^*)^3.$$

It is claimed that any binding energy-bond length relation of the form $E(a)$ can be cast into the universal form by scaling first the energy with its value at the minimum and then the length a by subtracting the equilibrium length and dividing by a scaling factor which is chosen to ensure that the second derivative $E''(a^*)$ is equal to unity. Rose *et al.* choose the Wigner-Seitz radius r_{WS} as their measure of length so that $a^* = (r_{\text{WS}} - r_{\text{WSE}})/l$, where r_{WSE} is the equilibrium value of r_{WS} and l turns out to be

$$\left[\frac{E_{\text{coh}}}{12\pi r_{\text{WSE}} K_0} \right]^{1/2}.$$

Given a set of energy-length relationships, one may scale the energies until all curves have a minimum in the ordinate at -1 , shift the curves so that the minimum falls in the abscissa at zero, and scale the lengths until all curves have the same second derivative. It is obvious that in the range where the variation of energy with length is quadratic, the curves will fall on a universal relationship. It is less obvious that the universality will extend well beyond the harmonic range. Since we have amassed a fairly large database of E - V points, it seemed appropriate to attempt to scale our data to the Rose equation of state, and the result is shown in Fig. 4. In Fig. 5 we show in several

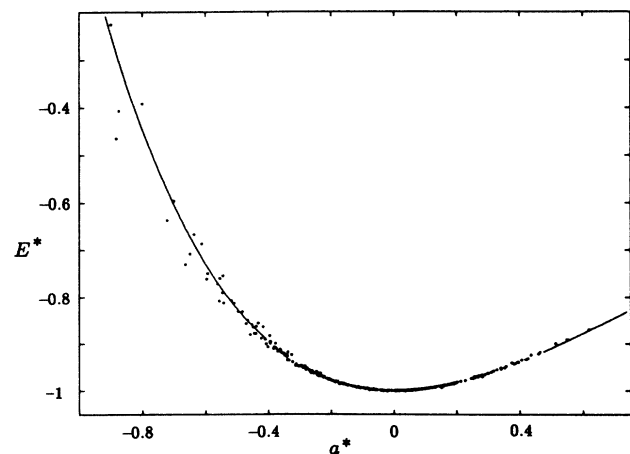


FIG. 4. Data points from Fig. 2 scaled to the Rose equation of state; E^* is the scaled binding energy and a^* the scaled Wigner-Seitz radius. The solid curve shown is the function $-(1+a^*)e^{-a^*}$.

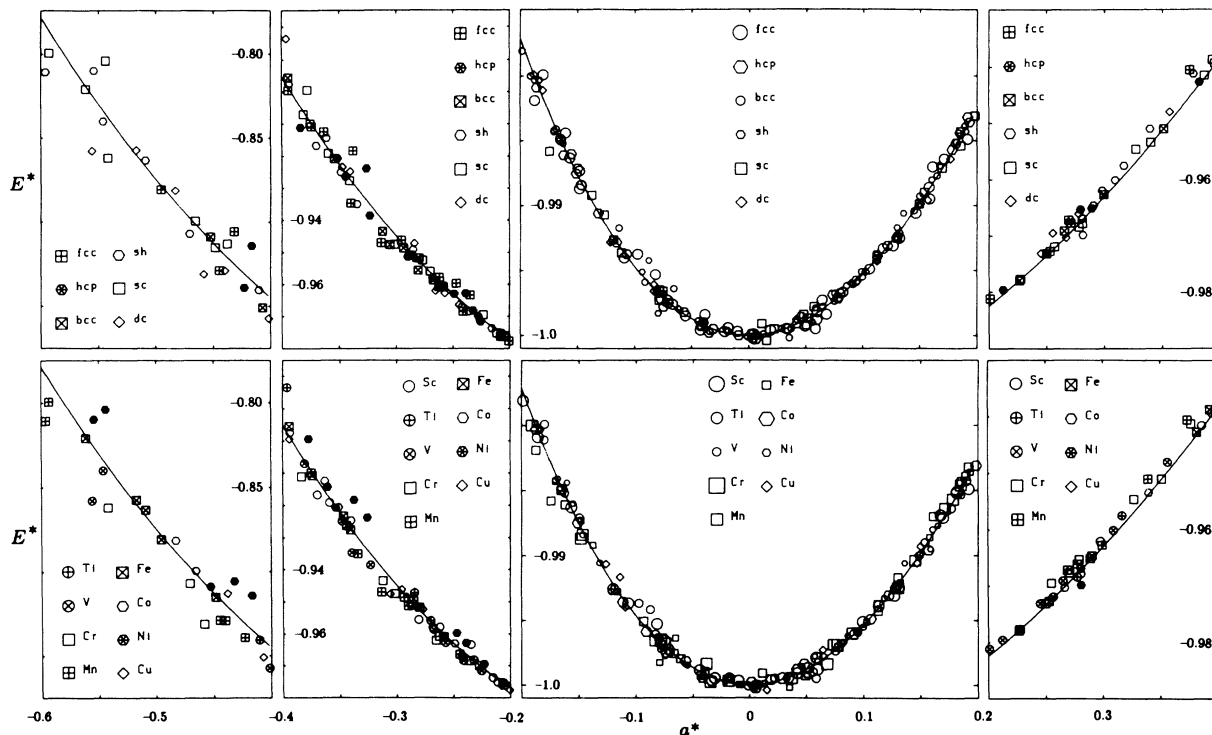


FIG. 5. Data from Fig. 4 shown on expanded scales so that each point may be identified with a particular element and crystal structure. Axes and the solid curve are as in Fig. 4. To avoid showing a lot of empty space, we have split the a^* axis into panels and used an optimal E^* scale for each panel. In the upper panels the points are labeled according to structure, and in the lower according to element. This illustrates in which cases there is deviation from the Rose equation of state.

panels the data on expanded scale—each panel appears twice, once with the points distinguished by structure and once by element. As expected, the fit is perfect close to the minimum, and any deviation here is due to errors in the least-squares procedure and a small amount of noise in the curves in Fig. 2. It is noticeable that our data deviate from universality in the high-pressure regime while the fit is excellent up to very large volumes. Unfortunately, the latter range is of little interest in practice. Note that the deviation at high pressure is mostly confined to the non-close-packed structures or to Ni. However, the deviations are not such that one can even draw a smooth curve through all the points of a given metal. Our data indicate that the universal scaling does not apply to all structures of all metals, or even to all structures of a given metal; but for one structure of one metal one can find a parameterization of the Rose equation of state that will go through all the points.^{25,26} Also the universal curve does fit over a range of a^* which is significantly beyond the harmonic range.

B. Transferability of tight-binding parameters

The fit to the Rose equation of state is good enough that we may take the analysis a little further. At the same time we will renew contact with tight-binding theory and make an assessment of the transferability of the tight-binding model into situations where close packing no longer pertains (e.g., vacancies, surfaces, etc.).

Rose *et al.*⁶⁶ did not offer any explanation of their remarkable result; in particular, they did not associate their length scaling parameter l very convincingly with any physical property of the metals in question. For example, replacing l by the Thomas-Fermi screening length led to a number of anomalies in the universality of the scaling procedure.⁶⁵ A very interesting analysis from the point of view of tight-binding theory was made by Spanjaard and Desjonquères.⁶⁷ They considered a tight-binding model for the d band with transfer integrals scaling with bond length R like $-e^{-qR}$ and a repulsive Born-Mayer-type of interaction of the form e^{-pR} . In the second-moment approximation, the binding energy can be written in closed form, having an attractive term proportional to $-\sqrt{Z}e^{-qR}$ and a repulsive term proportional to Ze^{-pR} , where Z is the number of neighbors. (This is also the motivation behind the Finnis-Sinclair^{68,69} interatomic potential for transition metals.) Spanjaard and Desjonquères were able to scale their binding-energy expression $E_B(R)$ to the form $E^*(R^*)$, where $R^* = (R - R_0)/l_{SD}$ if R_0 is the equilibrium bond length and l_{SD} related to the Rose *et al.* scaling length via $l_{SD}/l = r_{WSE}/R_0$. They then found a number of interesting consequences. (i) The curves of $E^*(R^*)$ were independent of the ratio p/q for all values between 2 and 5, except for deviations at large volumes. (ii) Using $p/q = 2.95$ the curve of $E^*(R^*)$ was indistinguishable from the Rose equation of state. (iii) The scaling procedure results in the following relation between the scal-

ing length and the tight-binding parameters:

$$l_{SD} = \frac{1}{\sqrt{pq}}.$$

Although this analysis is only possible in the second-moment approximation, it would be encouraging if the values of l_{SD} for a particular metal were fairly independent of structure, since this would imply that a tight-binding parameterization of p and q might be transferable. In Fig. 6, we show l_{SD} from our calculated $E-V$ curves, as well as the values obtained from the experimental bond lengths, cohesive energy, and bulk modulus. We find that, indeed, while l_{SD} varies from metal to metal, in many cases it has a universal value for all structures except the diamond cubic. This does not immediately lead to tight-binding parameters, since only the product pq is obtained. However, the decay of the transfer integrals q can be obtained for transition metals from quantum-mechanical arguments^{70,71,30,6}—one finds qR_0 varies between 3 and 5 (its canonical value) across the transition series. The Born-Mayer exponent is less easy to estimate, and it is this parameter which could be obtained from Fig. 6.

We have not made any tight-binding calculations of the structural $E-V$ relations. Therefore we do not know whether the usual canonical tight-binding d -band model is capable of reproducing the LDA results for non-close-packed structures. Having the curves in Fig. 2 available should make the problem easier. This, at least, was the case in Si. The original Chadi-Harrison^{72,73} tight-binding

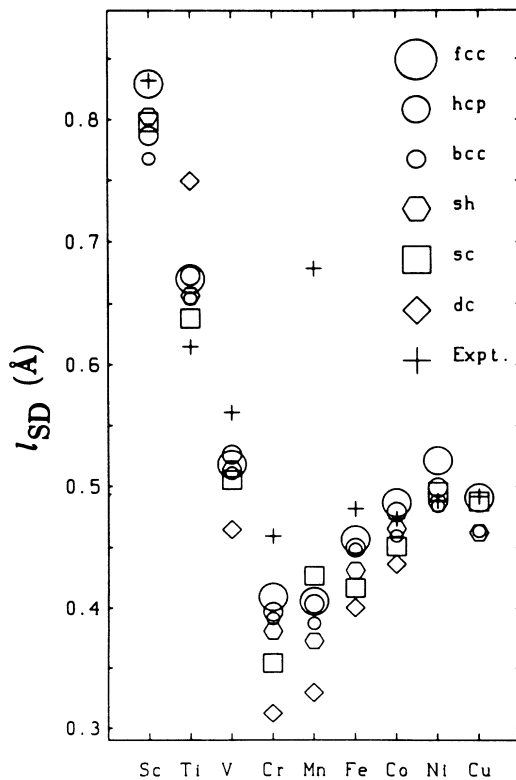


FIG. 6. The Spanjaard and Desjonquères scaling parameter l_{SD} (Å) calculated from data in Fig. 2 for each structure and for each element. Estimates from experimental cohesive energy, atomic volume, and bulk modulus are shown as crosses.

model for Si gave only moderate success compared to the LDA results for phase stability, and especially quite poor reproduction of the stability of close-packed phases.⁵⁵ Later, however, Goodwin *et al.*⁵⁶ used the LDA curves to actually make a fit to a scaling law for tight-binding parameters, leading to a tight-binding model for Si that reproduces the LDA results very well.

A particular criticism of the tight-binding method is that the diagonal Hamiltonian matrix elements are constant and do not vary with atomic volume or crystal structure. This leads, in Si, to large errors in deformation potentials, for example, and is probably the origin of the failure of the Chadi-Harrison model to reproduce the LDA results for close-packed structures. In the case of transition metals, we can address this question rather more easily. The canonical d -band model⁶ results in a Hamiltonian which is directly analogous to the first-order LMTO Hamiltonian,⁴⁰

$$H_{ij} = (C - E_v)_i \delta_{ij} + \sqrt{\Delta}_i S_{ij} \sqrt{\Delta}_j.$$

Here i and j are composite site and orbital indices, $C - E_v$ and $\sqrt{\Delta}$ are standard potential parameters, and S is the matrix of LMTO structure constants.^{19,40} Matrix elements in the second term, in the usual tight-binding model, take the Slater-Koster⁶ form

$$\begin{pmatrix} (dd\sigma) \\ (dd\pi) \\ (dd\delta) \end{pmatrix} = \begin{pmatrix} -60 \\ +40 \\ -10 \end{pmatrix} \times \Delta \left(\frac{s}{d} \right)^5,$$

in which the bandwidth is 25Δ , d is the bond length, and s is the Wigner-Seitz radius. The first term $C - E_v$ corresponds to ϵ_d (see Sec. III) and is taken to be the fixed-energy zero and center of the d band. Therefore, the volume and structure dependence enters only in the variation of the Slater-Koster parameters. For fixed-volume distortions, these scale like $1/d^5$, while the volume dependence of Δ (Refs. 70 and 6) is canceled by the s^5 so that the Slater-Koster integrals also account correctly for volume dilatations in the tight-binding model.⁷⁴ We show in Table IV self-consistent LMTO-ASA d -band potential parameters in vanadium for the fcc, bcc, and simple cubic structures at the reference atomic volume Ω_0 . The fact that $C - E_v$ and $\sqrt{\Delta}$ are nearly the same in a wide range of coordination numbers is encouraging, but the error involved in assuming a volume-independent band center remains to be assessed.

We believe, therefore, that it will be possible to construct tight-binding models for transition metals that will be transferable. The tight-binding method has many advantages: it is simple and transparent, and easy to carry out in both reciprocal and direct space.

TABLE IV. LMTO d -electron potential parameters for V in fcc, bcc, and sc lattices.

Structure	$C - E_v$ (Ry)	$\sqrt{\Delta}$ (Ry ^{1/2})
fcc	0.178	0.146
bcc	0.184	0.146
sc	0.203	0.171

VIII. DISCUSSION AND CONCLUSIONS

We have presented a systematic study of the structural energy-volume relations of first-row transition metals in the local-density approximation. This serves as a demonstration of the full-potential LMTO method^{17,27} as well as presenting a useful database for the field testing of interatomic potentials. The analysis has concentrated on the connection to simpler models and non-self-consistent calculations; particular emphasis has been placed on the hierarchy self-consistent LDA \rightarrow non-self-consistent LDA \rightarrow semiempirical tight binding. This connection has already been made in the literature, but only on a formal level. For example, Sutton *et al.*,⁷ while presenting the detailed justification of their tight-binding bond model using the Harris-Foulkes stationary functional, did not show comparisons between their bond, promotion and repulsive energies as estimated from empirical or canonical models, and the same quantities calculated exactly in the LDA. We have used the Rose equation of state^{65,66} and the Spanjaard and Desjonquères tight-binding analysis⁶⁷ to use our E - V database to address the question of transferability of tight-binding parameters. We have also argued that since the HF approximation is capable of reproducing very accurately the self-consistent calculations of static structural properties of transition metals, on the basis of the arguments of Sutton *et al.*⁷ it should be possible to find a tight-binding model suitable for defect calculations. [This is already known by experience; there have been numerous successful calculations of defect and surface structures of transition metals (see, for

example, Refs. 75 and 76).]

Little mention has been made of the class of empirical classical potentials such as the embedded-atom,⁷⁷ Finnis-Sinclair,⁶⁸ and "glue"⁷⁸ models, although we believe our energy-volume curves will be of some use in constructing such models in the future. These are all essentially of the same form, although their derivations are quite different. This has led to some confusion in evaluating their range of applicability. One could extend the hierarchy given in the previous paragraph one stage further by adding classical potentials as derivatives of the tight-binding scheme. This is implicit in the derivation of the Finnis-Sinclair potentials, although the embedded-atom method is thought to originate directly from self-consistent density-functional theory. The "glue" model, on the contrary, was constructed on a wholly *ad hoc* basis, but nonetheless it has been no less successful than the other two theories.^{78,79} We do not know whether these classical potentials can be given a firmer footing, nor whether the results presented here will be useful in doing so.

ACKNOWLEDGMENTS

We thank O. K. Andersen, N. E. Christensen, M. W. Finnis, and A. Liechtenstein for many helpful conversations. H. Skriver kindly supplied details of his calculations. We are grateful for financial support from the Max-Planck Gesellschaft, the UK Science and Engineering Research Council, and the U.S. Air Force Office of Scientific Research (AFOSR) under Contract No. F49620-85-K-0009.

*Present address: SRI International, 333 Ravenswood Avenue, Menlo Park, California 94025.

†Permanent address: Department of Physics, Aristoteles University of Thessaloniki, GR-54006, Greece.

¹P. C. Hohenberg and W. Kohn, *Phys. Rev.* **136**, B864 (1964).

²W. Kohn and L. Sham, *Phys. Rev.* **140**, A1133 (1965).

³J. Harris, *Phys. Rev. B* **31**, 1770 (1985).

⁴W. M. C. Foulkes, Ph.D. thesis, University of Cambridge, 1987.

⁵W. M. C. Foulkes and R. Haydock, *Phys. Rev. B* **39**, 12520 (1989).

⁶D. G. Pettifor, *J. Phys. F* **7**, 613 (1977).

⁷A. P. Sutton, M. W. Finnis, D. G. Pettifor, and Y. Ohta, *J. Phys. C* **21**, 35 (1988).

⁸M. W. Finnis, in *Chemistry and Physics of Fracture*, edited by R. M. Latanision and R. H. Jones (Nijhoff, Dordrecht, 1987), p. 177.

⁹M. W. Finnis, A. T. Paxton, D. G. Pettifor, A. P. Sutton, and Y. Ohta, *Philos. Mag. A* **58**, 143 (1988).

¹⁰J. W. Christian, *The Theory of Transformations in Metals and Alloys*, 2nd ed. (Pergamon, Oxford, 1975), Ch. 5.

¹¹*Many-Atom Interactions in Solids*, edited by R. M. Nieminen, M. J. Puska, and M. Manninen (Springer, Berlin, 1990).

¹²M. W. Thompson, *Defects and Radiation Damage in Metals* (Cambridge University Press, Cambridge, England, 1969).

¹³V. Vitek, *Crystal Latt. Def.* **5**, 1 (1974).

¹⁴A. P. Sutton and V. Vitek, *Philos. Trans. R. Soc. London, Ser. A* **309**, 1 (1983).

¹⁵P. Bagno, O. Jepsen, and O. Gunnarsson, *Phys. Rev. B* **40**, 1997 (1989).

¹⁶O. K. Andersen, *Phys. Rev. B* **12**, 3060 (1975).

¹⁷M. Methfessel, *Phys. Rev. B* **38**, 1537 (1988).

¹⁸O. K. Andersen, *Solid State Commun.* **13**, 133 (1973).

¹⁹O. K. Andersen, in *Electronic Structure of Complex Systems*, edited by P. Phariseau and W. M. Temmerman (Plenum, New York, 1984), p. 11.

²⁰D. J. Chadi and M. L. Cohen, *Phys. Rev. B* **8**, 5747 (1973).

²¹L. F. Mattheiss and D. R. Hamann, *Phys. Rev. B* **33**, 823 (1986).

²²V. L. Moruzzi, J. F. Janak, and A. R. Williams, *Calculated Electronic Properties of Metals* (Pergamon, New York, 1978).

²³Zhi-Wei Lu, D. Singh, and H. Krakauer, *Phys. Rev. B* **36**, 7335 (1987).

²⁴C.-L. Fu and K.-M. Ho, *Phys. Rev. B* **28**, 5480 (1983).

²⁵N. Takeuchi, C. T. Chan, and K.-M. Ho, *Phys. Rev. B* **40**, 1565 (1989).

²⁶B. J. Min and K.-M. Ho, *Phys. Rev. B* **40**, 7532 (1989).

²⁷M. Methfessel, C. O. Rodriguez, and O. K. Andersen, *Phys. Rev. B* **40**, 2009 (1989).

²⁸M. Methfessel and A. T. Paxton, *Phys. Rev. B* **40**, 3616 (1989).

²⁹D. G. Pettifor, *J. Phys. C* **3**, 367 (1970).

³⁰F. Ducastelle and F. Cyrot-Lackmann, *J. Phys. Chem. Solids* **32**, 285 (1971).

³¹D. G. Pettifor, in *Metallurgical Chemistry*, edited by O. Kubachewski (Her Majesty's Stationery Office, London, 1972), p. 191.

- ³²O. K. Andersen and O. Jepsen, *Physica B+C* (Amsterdam) **91B**, 317 (1977).
- ³³S. Glanville, A. T. Paxton, and M. W. Finnis, *J. Phys. F* **18**, 693 (1988).
- ³⁴J. Friedel, *Trans. AIME* **230**, 616 (1964).
- ³⁵G. Allan, *Ann. Phys. (Paris)* **5**, 169 (1970).
- ³⁶J. Friedel, *J. Phys. Paris* **39**, 651 (1978).
- ³⁷D. G. Pettifor, in *Solid State Physics*, edited by H. Ehrenreich, F. Seitz, and D. Turnbull (Academic, New York, 1987), Vol. 40, p. 43.
- ³⁸J. C. Slater and G. F. Koster, *Phys. Rev.* **94**, 1498 (1954).
- ³⁹H. Skriver, *Phys. Rev. B* **31**, 1909 (1985).
- ⁴⁰O. K. Andersen, O. Jepsen, and D. Glötzel, in *Highlights of Condensed Matter Theory*, edited by F. Bassani *et al.* (North-Holland, Amsterdam, 1985), p. 59.
- ⁴¹A. T. Paxton, in *Atomistic Simulation of Materials*, edited by V. Vitek and D. J. Srolovitz (Plenum, New York, 1989), p. 327.
- ⁴²A. K. Sinha, *Prog. Mater. Sci.* **15**, 81 (1972).
- ⁴³F. C. Frank and J. S. Kaspar, *Acta Crystallogr.* **12**, 483 (1959).
- ⁴⁴J. S. Kaspar and B. W. Roberts, *Phys. Rev.* **101**, 537 (1956).
- ⁴⁵L. D. Blackburn, L. Kaufman, and M. Cohen, *Acta Metall.* **13**, 533 (1965).
- ⁴⁶R. L. Clendenon and H. G. Drickamer, *J. Phys. Chem. Solids* **25**, 865 (1964).
- ⁴⁷C. S. Wang, B. M. Klein, and H. Krakauer, *Phys. Rev. Lett.* **54**, 1852 (1985).
- ⁴⁸D. C. Langreth and M. J. Mehl, *Phys. Rev. Lett.* **47**, 446 (1981).
- ⁴⁹A. R. Troiano and J. L. Tokich, *Trans. AIME* **175**, 728 (1949).
- ⁵⁰C. Bonelle and F. Vergand-Jacquot, *C. R. Acad. Sci. Paris* **252**, 1448 (1961).
- ⁵¹P. Hemminger and H. Weik, *Acta Crystallogr.* **19**, 690 (1965).
- ⁵²I. Teodorescu and A. Glodeanu, *Stud. Cerc. Fiz. Romin.* **112**, 331 (1960).
- ⁵³M. T. Yin and M. L. Cohen, *Phys. Rev. B* **26**, 5668 (1982).
- ⁵⁴R. Biswas and D. R. Hamann, *Phys. Rev. Lett.* **55**, 2001 (1985).
- ⁵⁵A. T. Paxton, A. P. Sutton, and C. M. M. Nex, *J. Phys. C* **20**, L263 (1987).
- ⁵⁶L. Goodwin, A. J. Skinner, and D. G. Pettifor, *Europhys. Lett.* **9**, 701 (1989).
- ⁵⁷Overestimation of K_0 is a consequence of the underestimation of atomic volume. The error is lessened if K_0 is calculated at the experimental atomic volume. This paper is primarily concerned with models for transition metals which may be applied, for example, in molecular-dynamics calculations; therefore it is appropriate to discuss equilibrium features of the model rather than to obtain the best agreement with experiment.
- ⁵⁸J. R. Chelikowsky and S. G. Louie, *Phys. Rev. B* **29**, 3470 (1984).
- ⁵⁹M. W. Finnis, *J. Phys. Condens. Matter* **2**, 331 (1990).
- ⁶⁰H. M. Polatoglou and M. Methfessel, *Phys. Rev. B* **41**, 5898 (1990).
- ⁶¹M. Methfessel and J. Kübler, *J. Phys. F* **12**, 141 (1982).
- ⁶²H. M. Polatoglou and M. Methfessel, *Phys. Rev. B* **37**, 10403 (1988).
- ⁶³M. Weinert and R. E. Watson, *Phys. Rev. B* **29**, 3001 (1984).
- ⁶⁴J. G. Wright and J. Goddard, *Philos. Mag.* **11**, 485 (1965).
- ⁶⁵J. H. Rose, J. Ferrante, and J. R. Smith, *Phys. Rev. Lett.* **47**, 675 (1981).
- ⁶⁶J. H. Rose, J. R. Smith, F. Guinea, and J. Ferrante, *Phys. Rev. B* **29**, 2963 (1984), and references therein.
- ⁶⁷D. Spanjaard and M. C. Desjonquères, *Phys. Rev. B* **30**, 4822 (1984).
- ⁶⁸M. W. Finnis and J. E. Sinclair, *Philos. Mag. A* **50**, 45 (1984).
- ⁶⁹G. J. Ackland, M. W. Finnis, and V. Vitek, *J. Phys. F* **18**, L153 (1988).
- ⁷⁰V. Heine, *Phys. Rev.* **153**, 673 (1967).
- ⁷¹F. Ducastelle, *J. Phys. (Paris)* **31**, 1055 (1970).
- ⁷²D. J. Chadi, *Phys. Rev. Lett.* **41**, 1062 (1978).
- ⁷³W. A. Harrison, *Phys. Rev. B* **27**, 3592 (1983).
- ⁷⁴In Si the bandwidth scales like $1/d^2$ so that the Slater-Koster parameters must have the same length dependence. Unfortunately these are not short-ranged, as they are in metals. On the other hand, short-ranged tight-binding parameters do not benefit from this cancellation and require an explicit volume-dependent correction (see Refs. 40, 41, and 55).
- ⁷⁵B. Legrand, *Philos. Mag. A* **52**, 83 (1985).
- ⁷⁶B. Legrand, G. Treglia, M. C. Desjonquères, and D. Spanjaard, *J. Phys. C* **19**, 4463 (1986).
- ⁷⁷M. S. Daw and M. I. Baskes, *Phys. Rev. B* **29**, 6443 (1984).
- ⁷⁸F. Ercolessi, E. Tosatti, and M. Parrinello, *Phys. Rev. Lett.* **57**, 719 (1986).
- ⁷⁹F. Ercolessi, M. Parrinello, and E. Tosatti, *Philos. Mag. A* **58**, 213 (1988).